A Novel Adaptive Topology for Photovoltaic Array under Partial Shadings to Increase Energy Yields

G. Meerimatha[a‡], B. Loveswara Rao[b],

[a, b]Department of Electrical and Electronics Engineering, Koneru Lakshmaiah Education Foundation,

Vaddeswaram, Guntur, A.P, INDIA.

(gmeerimatha2k9@gmail.com, loveswararao@kluniversity.in)

‡Corresponding Author; G. Meerimatha, KLEF, Tel: +91-9440333831,

gmeerimatha2k9@gmail.com

Received: 05.06.2020 Accepted:01.07.2020

Abstract-This paper proposed a new adaptive reconfiguration technique for total-cross-tied (TCT) PV array to reduce the loss of mismatch and to increase energy output under partial shadings (PS) through MATLAB-SIMULINK. During this work, the electrical connections between PV modules are modified with the help of proposed pattern search algorithm to maintain equal currents in each row on the basis of shading conditions, thus increasing the current of the array. The proposed algorithm classifies the possible number of PV array connections for adaptive system and determines the optimal connection between them. This approach is implemented on a 3×3 array and evaluated under various possible conditions of shadings. In contrast, this proposed method is validated with current reconfiguration methods and compares the global maximum power point (GMPP), shadow loss, efficiency and fill factor. Based on the findings of this study, it is acknowledged that the proposed adaptive method improved the power output of TCT array by 9.6% compared to other methods under partial shadings.

KeywordsAdaptive PV array; Dynamic reconfiguration; Global peak (GP); Pattern search algorithm (PSA).

1. Introduction

Renewable Energy Source (RES) integration significantly alters the period of conventional power systems by improving power generation efficiency and fulfilling global demand. Photovoltaic (PV) energy installs quickly among the RES and produces enough energy in a short time [1]. In addition, the cost of PV material is reduced on a daily basis compared to other renewables. Despite the popularity of PV technology, there are few factors that can control PV output, including solar insolation, ambient temperature, snowfall, and aging [2]. Variations in PV module irradiance may cause partial shading (PS) in the PV array; further, this effect may trigger loss of mismatch by disturbing the I-V characteristics of individual PV modules. As a result, considerable power loss in the PV system and a mitigation technique is required to cut back these losses. Various PV array connection schemes are proposed and implemented earlier in the literature, such as simple-series (SS), parallel (P), series-parallel (SP), total cross-tied (TCT), bridge-link (BL), honey-comb (HC), in order to harness maximum power under mismatch conditions [3-4]. In [4], the authors modelled PV array connections using Simulink on the 6×6 size of an array under the row, column, and diagonal shading conditions. The examined connections are SS, SP, TCT, BL, and HC. In this work, the global power output, power loss, and fill-factor are compared from the PV arrays to discover the best connection, which is capable of generating the highest maximum power. Based on the study, it has been identified that the TCT connection provides better power output under PS compared to other connections. In [5], the authors adopted a 5×5 array to test the effects of PS on SS, P, SP, TCT, BL, and HC PV array connections. In this work, various shading scenarios are created using Matlab-Simulink and compare PV arrays performances using theoretical parameters. The inference of this paper is that the TCT connection improved power output compared to other connections under PS. From the method of array connections, it is understood that the TCT array eliminates the loss of mismatch during PS and displays the highest

output power than the other connections. However, TCT has one major downside of restricting the array output current based on shaded modules in a row [6]. As a consequence, there are several peak points in the PV output characteristics. The way to minimize multiple peaks in a TCT connection is by maintaining the same current in each row, which occurs only when dynamic reconfiguration appears in the TCT array [7]. Dynamic reconfiguration is a process that dynamically connects PV modules to spread shading effects and preserve equal currents in each row under PS, thereby increase maximum power output [7].

In [8], the authors suggested Electrical Array Reconfiguration (EAR) to achieve higher power output in a 3×3 TCT array under the effect of PS. In this method, the PV module connections dynamically altered based on shading conditions. Under PS, the proposed EAR method identifies a unique connection that can distribute shadings equally in each row to improve power output. The essential requirement of this method is that it requires more sensors and switches. As a result, this entire operation is quite tricky. In [9], a novel adaptive technique based on a fuzzy algorithm is proposed to satisfy the load current. The proposed algorithm senses defective and shading modules based on the measurement of current and combine these shaded modules in parallel groups using switches that can satisfy the request for the load. This method is assessed on a 3×3 array, which includes both voltage and current sensors required for each module; this would increase the cost of the PV system. A similar method is presented in [10]. In this work, the authors proposed a dynamic reconfiguration method for 4×3 TCT array to improve output current under PS. The proposed system consists of upper, middle, and lower layers. Each layer is fastened with three switches. If shading occurs in any layer of the modules, the switches are connected in such a way as to retain the same current in rows to increase the array output current. The problem with this method is that the system installation is very difficult in real-time. In [11], a scanning algorithm based reconfiguration method is proposed for 4×3 TCT array to improve power output under the effect of PS. This reconfiguration consists mainly of three parts, such as adaptive, fixed, and switching matrix. The switching matrix configuration is such that the adaptive modules connected to the fixed modules compensate for the irradiance drop in each row under PS, thereby increasing the array's power output. This work requires an $m+1$ number of sensors and double-pole single through (DPST) switches to perform this experiment. The irradiance equalization technique for the 4×4 TCT array under the influence of PS is demonstrated in [12]. Irradiance equalization is the sum of the irradiance in each row equal to the average radiance of the array. In this work, the authors used sorting algorithms to sort out the PV modules, whose irradiances are very similar in each row. Besides, this algorithm selects the optimum connection and provides control signals for connecting modules to the switches, thus improving power output. This approach has the downside of manually adjusting the irradiance of PV modules for each iteration. In [13], a novel dynamic method is proposed for 4×4 TCT array to create individual rows using a switching matrix, whose irradiance levels are identical under PS. Two algorithms, i.e., random search and deterministic, are developed in this paper to control the dynamic operation between PV modules within the array. In this work, each algorithm forms an array by creating rows of identical irradiance. Finally, the algorithms choose an optimal connection based equalization index (EI), which is capable of distributing shading effects and improving power output under PS. In [14], an optimal reconfiguration is proposed to minimize the irradiance mismatch across each row in the TCT array. This problem is formulated using a non-linear optimization technique and solved by branch and bound (BB) algorithm to address this issue. During this work, the shaded modules are reconfigured from one position to another with the aid of switches under PS to achieve equal irradiance in each row of the array. However, this method needed more number of switches and sensors to carry out this experiment. In [15], proposed a Dynamic PV array (DPV) strategy to reduce repetitive shading effects and increase power efficiency. A dynamic algorithm is proposed in this work to determine whether the PV array is experienced shading or not based on the measurement of module currents. Under PS, the algorithm identifies the optimal connection and transmits the signals to the switches to communicate between PV modules to increase array power output. For each module, this approach needs a switch; this will increase the cost of the system. A variation of this method is proposed in [16]. In this work, the authors proposed a one-time arrangement pattern, namely magic-square (MS), to mitigate PS loss and improve the power output of the TCT array. This MS arrangement is implemented on a 3×3 array by shifting the module's physical locations without modifying their electrical connections. The results of this paper revealed that the proposed method enhanced power output as compared to other connections. Based on the literature report, two main observations are notified, which includes; (i) the dynamic reconfiguration method can improve the maximum power of the TCT array under PS. (ii) The existed dynamic reconfiguration methods facing many challenges while searching for the optimum connection due to system complexity, difficulty in switching operations, large computational time, inclusion of more sensors and other electronic components. In order to address all these issues, a novel adaptive reconfiguration method is proposed for TCT array in this paper based on pattern search algorithm to improve maximum power under partial shadings. The proposed system consists of mainly three components such

as fixed part, adaptive part, and switching matrix. In [16], the authors used a magic-square method by physically switching the positions of the modules in the TCT array without altering their electrical connections. It is a challenging job to modify the physical positions of the PV modules at the time of operation. In proposed method, the PV module's locations do not change, but their electrical connections are modified based on shading effects to achieve the identical row currents. This proposed method, however, requires a few sensors and a comfortable switching matrix compared with other methods reported in the literature [11-12]. The proposed algorithm identifies a possible number of connections in this work that connect adaptive modules to the fixed part modules. Also, it decides the optimal connection between them based on the current variation index (CVI), which can deliver highest maximum power output under PS. This proposed method is tested under different shading conditions on a 3×3 TCT array and validated with the existing magic-square method [16] by obtaining global maximum power output (GMPP), fill factor (FF), efficiency and shadow loss (SL).

2. Photovoltaic (PV) Modeling

A PV model is essentially a semiconductor material whose p-n junction is exposed to the sunlight. Photovoltaic cells consist of several kinds of semiconductors, utilizing various material forms. In the present case, monocrystalline and polycrystalline silicon materials are commonly used in the industries to design single diode and two diode PV cell models. The single diode model, as per the literature, is more accurate for evaluating a PV system's output characteristics than the two diode model. Therefore, this paper considered a single diode model to look into the adaptive reconfiguration method. Fig.1 shows various types of single diode PV cells models such as ideal, Rs and Rp.

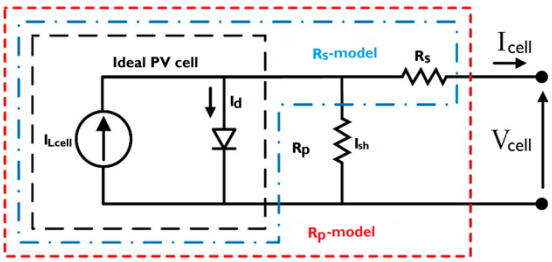

Fig.1. Single diode PV cell model.

The output I-V characteristics of a single PV cell can be written as,

$$I_{cell} = I_L - I_d\left[\exp\left(\frac{q\left(V_{cell}+I_{cell}R_s\right)}{akT}\right)-1\right]-\left(\frac{V_{cell}+I_{cell}R_s}{R_{sh}}\right) \quad (1)$$

In order to form a module, the considerable PV cells are connected in a series fashion. It can increase a module's output voltage rating in comparison to the single PV cell. The output I-V equation for the PV module is given as,

$$I_{pv} = I_L - I_d\left[\exp\left(\frac{q\left(V_{pv}+I_{pv}R_S\right)}{n_s akT}\right)-1\right]-\left(\frac{V_{pv}+I_{pv}R_S}{R_{SH}}\right) \quad (2)$$

It is noted from the above equation that the current produced by the module is closely related to the sunlight (I_L), which can be written as;

$$I_L = \frac{G}{G_{ref}}\left[I_{sc}\left(1+K_{isc}\left(T_c - T_{ref}\right)\right)\right] \quad (3)$$

The construction of the PV array is by combining the PV modules in series and parallel connection. The output functions of the PV array can be summarized as follows:

$$I_a = N_{pp}\left\{I_{ph} - I_0\left[\exp\left(\frac{V_a + I_a R_s}{V_t N_{ss}}\right)-1\right]\right\}-\left(\frac{V_a + I_a R_s}{R_p}\right) \quad (4)$$

The derived PV cell, module, and array mathematical equations can also be used to represent the performance characteristics under various irradiation and temperature, as shown in Fig.2 and Fig.3, respectively. The specifications of a PV module at Standard Test Condition (STC) are reported in Table 1.

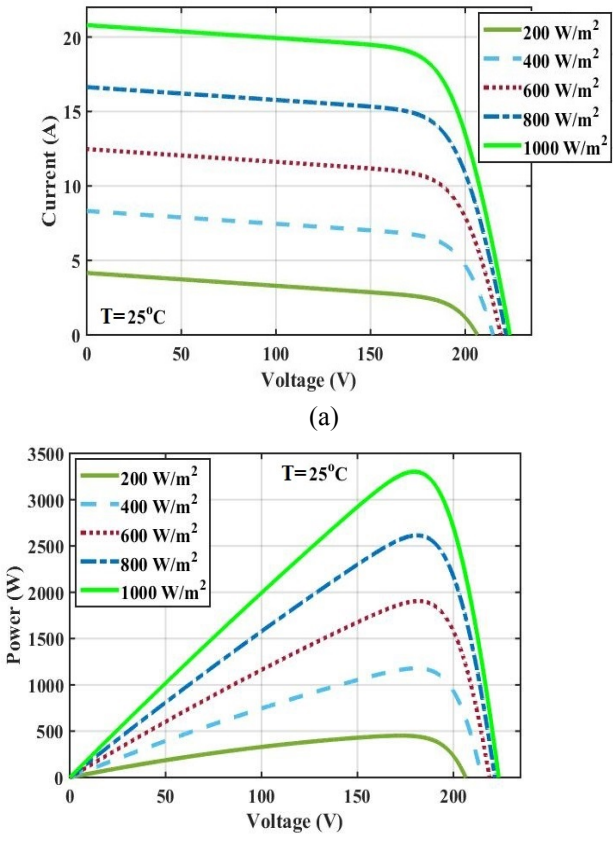

Fig. 2. (a) I-V curve, (b) P-V curve of 5×4 PV array at various Irradiance levels.

3. TCT PV array Modelling

TCT connection is a combination of parallel-connected PV modules as a row and series-connected rows referred to as a string. The TCT connection general topology is shown in Fig.4. The benefit of the TCT connection is that it provides a higher power output under PS than other connections [6]. Fig.4, it is showed that the PV modules are connected in parallel to form the rows. In row-wise connection, the individual module current is summed up; this can be obtained as,

$$I_a = \sum_{q=1}^{3}\left(I_{pq} - I_{(p+1)q}\right) \qquad (5)$$

where p and q are the row and column of the array. Eq. (5) can be referred to the TCT array output current. The array voltage is equal to the addition of individual row-wise voltages; this can be found by using Eq.(6). Note: In TCT connection, the voltage across each row is identical, equal to the module's maximum voltage. Where V_{mp} is module voltage with respect to p^{th} row.

$$V_a = \sum_{p=1}^{3} V_{mp} \qquad (6)$$

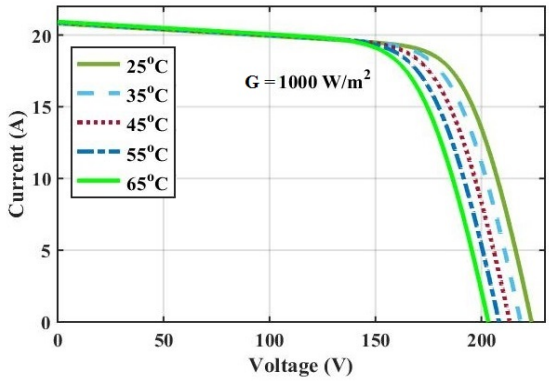

(a)

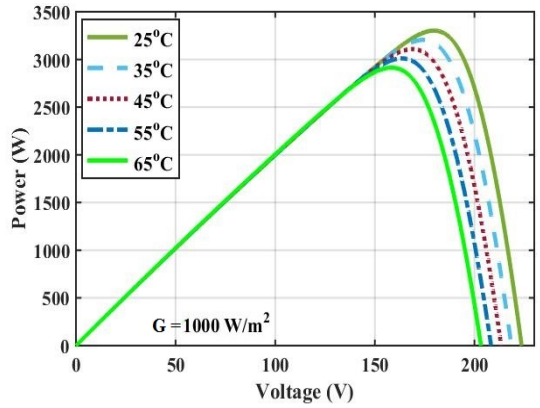

(b)

Fig.3. (a) I-V curve, (b) P-V curve of 5×4 PV array at various temperature levels.

Table 1. Modeling parameters of the PV module.

Parameters	Ratings
PV Power (P_{mp})	170.05W
Nominal Voltage (V_{oc})	44.2 V
Nominal Current (I_{sc})	5.2 A
Module Maximum Current(I_{mp})	4.75 A
Module Maximum Voltage(V_{mp})	35.8 V
PV Module Area	62.2inc×31.9inc

4. Proposed Adaptive System

The formation of the proposed system is explained in this section. The architecture of this adaptive system is shown in Fig.5. It contains a fixed part, an adaptive part, and a matrix for switching. The fixed part connection made like a sturdy within the 3×2 array size, which is the same as TCT. In the fixed part, F_1, F_2, and F_m are the sequentially connected rows. Throughout the process, the electrical connections of the fixed part do not change. In the adaptive, there is a parallel attachment of m number of PV modules to each row of a fixed part. The number of adaptive modules, as can be shown, is equal to the rows of the fixed part.

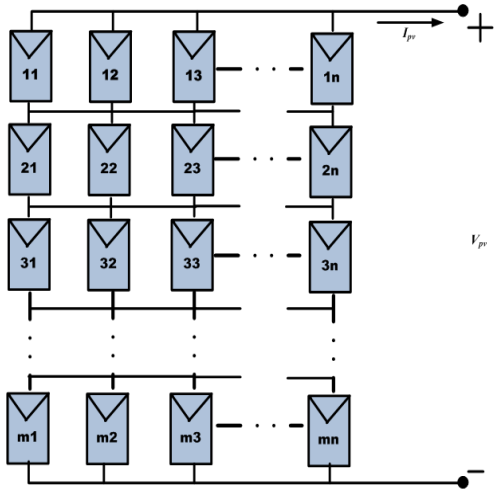

Fig. 4. TCT PV array Interconnection.

A switching matrix is the main core of this adaptive system; the structure can be seen in Fig.6. This operation is to provide S_{11}, S_{12}... S_{mm} switches to connect the PV modules from the adaptive part to the rows of the fixed part to increase the output power. Compared to the other methods provided in the literature [10-11], this proposed method needed *2.m.m* switches for the operation. Under normal conditions, the adaptive module is connected directly to the fixed part of the modules to receive the higher output power. Under PS, the number of adaptive modules connected to the fixed section is dependent on each row of the array's short-circuit currents (SCCs).

The principal of the proposed method is the forming of array rows using the modules whose insolation levels are similar to each other. This would trigger identical current levels at these rows, meaning that the current limiting issue would not suffer from the series connection of rows. As the solar insolation directly affects the current of a module, if the adaptive modules are connected through switches to the fixed part in such a way that the output currents of each row are

very similar, the PV array's output power will increase. The proposed pattern search algorithm triggered this entire adaptive process, which is demonstrated in the next section.

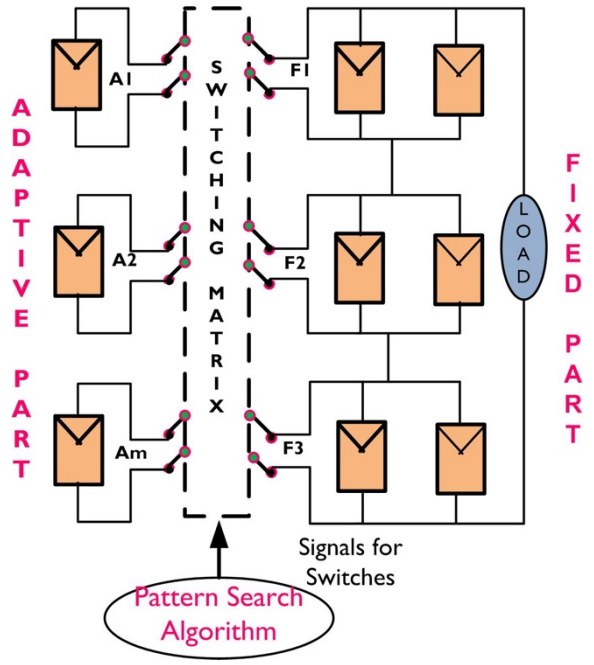

Fig. 5. Adaptive Reconfiguration Structure.

5. Pattern Search Algorithm

A pattern search algorithm is proposed in this paper to construct the rows of PV modules whose solar insolation levels in the TCT array are far closer with the help of electrical switching. The algorithm operation is divided into three loops, which are illustrated as follows;

I. First, the algorithm uses permutation and combination rules to find the possible number of connections that bind adaptive modules to the fixed part rows. According to the algorithm, the obtained possible connections for 3×3 PV array is m^m, i.e., 27, where m=3. (Note: Any adaptive module can connect to the fixed part only once, as per the algorithm.)

II. Second, in all possible connections, the algorithm estimates the short-circuit currents of each row of both adaptive and fixed part modules. At the end of each node, current sensors are mounted for measuring the output current of an adaptive system. According to the literature [11-15], different sensors, such as irradiance, current, and voltage, are used to calculate the parameters for reconfiguration inputs. Compared to [11-15], the proposed method employed only current sensors of *2.m*. Current sensor costs are relatively less when compared to sensors of irradiance type [15].

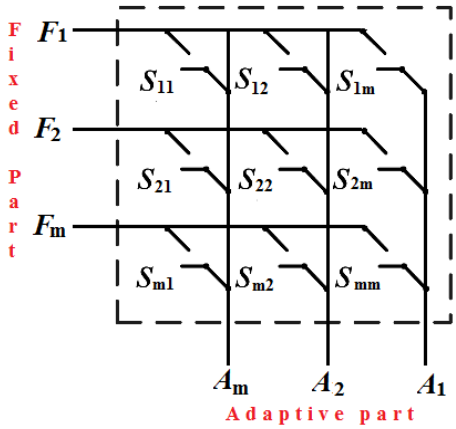

Fig. 6. Switching Matirx for reconfiguration.

III. In the third loop, the algorithm searches for the optimum one among possible connections based on the current variation index (CVI) given in Eq. (10). CVI is an index, which measures the row current differences in the array. Using Eq. (10), the algorithm calculates CVI for every possible connection and selects the connection with a lower CVI index as an optimum that can generates the highest output power. Finally, the algorithm sends a signal to the switches to bind adaptive modules to the fixed part according to the optimum connection. Where $I_s(Row_p)$ is the sum of adaptive and fixed module currents in a row, *Max I* and *Min I* are thehighest and lowest currents generated by the array. The flowchart of the pattern search algorithm is shown in Fig.7.

$$I_s(Row(p)) = I_s(F_p) + \sum I_s(A) \quad (7)$$

$$Max\ I = Max[I_{s_1}, I_{s_2} \ldots I_{s_m}] \quad (8)$$

$$Min\ I = Min[I_{s_1}, I_{s_2} \ldots I_{s_m}] \quad (9)$$

$$CVI = Max\ I - Min\ I \quad (10)$$

5.1. Description of PSCs

In order to test the effectiveness of this proposed method, three possible shading conditions are considered in this paper, such as a row, column and diagonal. For each shading, the proposed algorithm finds the optimum connection with the help of switching matrix and simulated I-V and P-V features.

5.2. Index Parameters

This paper focuses on three index parameters to check the achievement of the proposed system, such as the global maximum power point (GMPP), fill-factor (FF), efficiency

and shadow loss (SL). The numerical description of these parameters is expressed in [5].

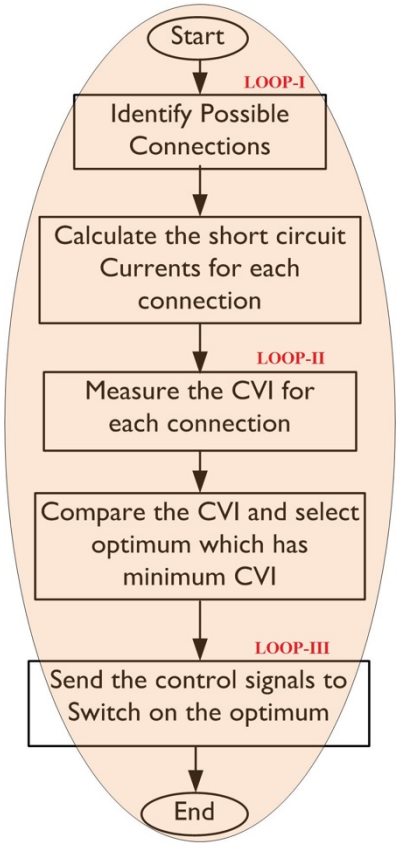

Fig.7. Flowchart of the proposed algorithm.

6. Results and Discussions

An adaptive method is proposed for TCT array to mitigate the effect of PS and improve the maximum power output. This method is implemented on 3×3 size of an array using Matlab-Simulink and tested under the possible row, column, and diagonal shading conditions. In addition to this, the proposed method is validated by obtaining GMPP, fill factor, and shadow loss under shading conditions using the magic-square [6] method.

6.1. Performance of Row Shading

The modules in the first two rows of both adaptive and fixed sections are partially shaded in row shading, with varying solar insolation, such as light-blue (400 W/m^2), and light-orange (600 W/m^2), grey (800 W/m^2), respectively, is shown in Fig.8 (a). The consumed irradiance of remaining modules in the adaptive system is 1000 W/m^2. Under that shading, for the adaptive system, the possible number of connections is 27. The obtained CVI index is calculated for each possible connection and is presented in Table.2. It is observed from the table that connection **6** is produced less CVI than other connections, so this connection provided the highest power output. Table 3 reported selected random connections and generated power output for this row shading. The positioning of adaptive modules in the fixed part of connection 6 is that A_2 is connected to F_1, A_1 is connected to F_2, and A_3 is connected to F_3. The global peak (GP) location of an optimal connection of a proposed method can be obtained by measuring the voltage and current using Eqs. (5)-(6). In addition, the simulated I-V and P-V curves are plotted to verify the GP for the reconfiguration methods, as shown in Fig.9. The parameters such as GMPP, fill-factor, efficiency and shadow loss are estimated from the figures and represented in Fig.12. It is observed from the shading results that the proposed adaptive system is increased power output as compared to other PV arrays.

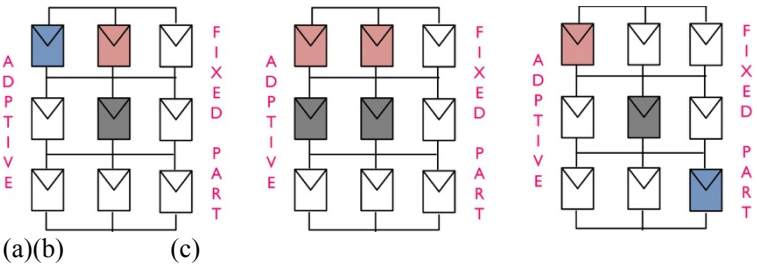

Fig. 8. Shadings: (a) Row shading, (b) Column shading, and (c) Diagonal shading.

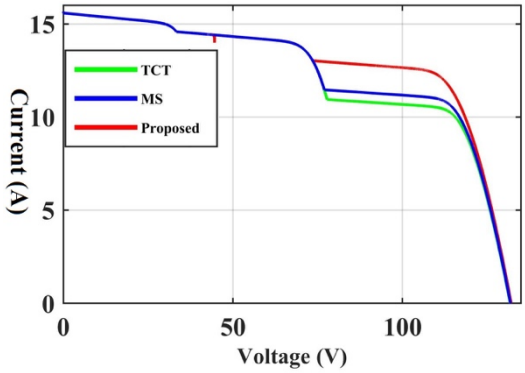

(a)I-V characteristics

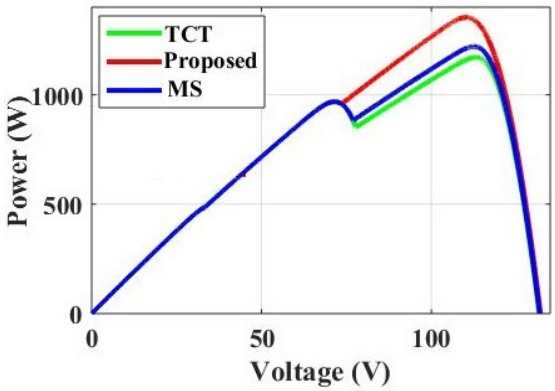

(b)P-V characteristics

Fig.9. Performance characteristics for Row-wise shading.

6.2.Performance of Column Shading

The modules in the first two columns of both adaptive and fixed sections are partially shaded in column shading, with varying solar insolation, such as light-orange (400W/m2), grey (800W/m^2) and light-orange (400W/m^2), grey (800W/m^2), respectively, is shown in Fig.8 (b). The consumed irradiance of remaining modules in the adaptive system is 1000 W/m^2. Under that shading, for the adaptive system, the possible number of connections is 27. Table 4 shows randomly selected connections and generated power output under the column shading. It is observed from the table that connection **15** is produced less CVI than other connections, so this connection provided the highest power output. The positioning of adaptive modules in the fixed part of connection 15 is that A_1 is connected to F_1, A_2 is connected to F_2, and A_3 is connected to F_3.

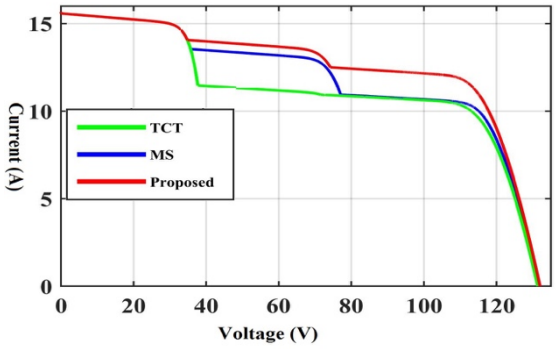

(a)I-V characteristics

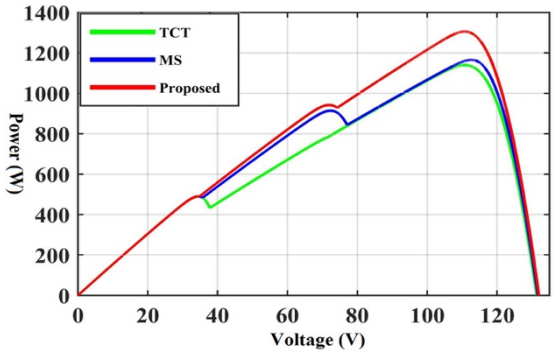

(b) P-V characteristics

Fig.10. Performance characteristics for Column-wise shading.

The global peak (GP) location of an optimal connection of a proposed method can be obtained by measuring the voltage and current using Eqs.(5)-(6). In addition, the simulated I-V and P-V curves are plotted to verify the GP for the reconfiguration methods, as shown in Fig.10. The parameterssuch as GMPP, fill-factor, efficiency and shadow loss are estimated from the figures and represented in Fig.12. It is observed from the shading results that the proposed adaptive system is increased power output as compared to other PV arrays.

6.3 Performance of Diagonal Shading

In this condition, the modules of both adaptive and fixed sections are partially shaded in a diagonal fashion, with varying solar insolation, such as light-orange (600 W/m^2) and grey (800 W/m^2), light blue (400 W/m^2), respectively, is shown in Fig.8(c). The consumed irradiance of remaining modules in the adaptive system is 1000 W/m^2. Under that shading, for the adaptive system, the possible number of connections is 27. Table 5 shows randomly selected connections and generated power output for the diagonal shading. It is observed from the table that connection **16** is produced less CVI than other connections, so this connection provided the highest power output.

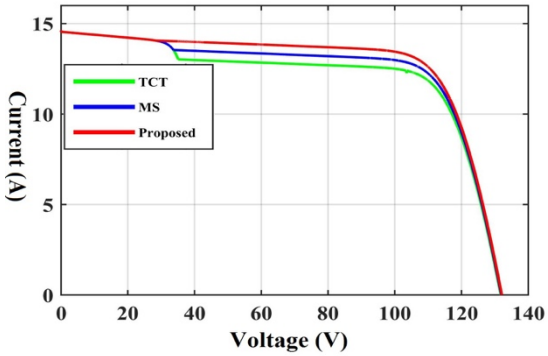

(a) I-V characteristics

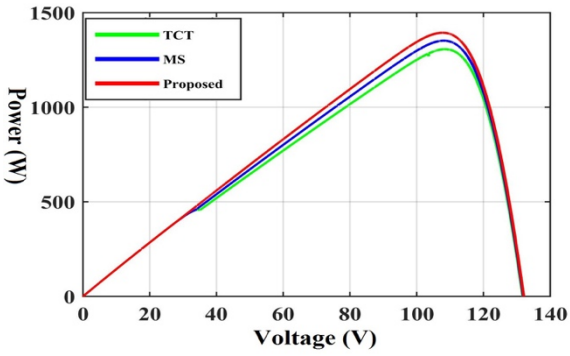

(b)P-V characteristics

Fig.11. Performance characteristics for diagonal type shading

The positioning of adaptive modules in the fixed part of connection 16 is that A_3 is connected to F_1, A_1, A_2 is connected to F_2, and no adaptive module is connected to F_3. The global peak (GP) location of an optimal connection of a proposed method can be obtained by measuring the voltage and current using Eqs. (5)-(6). In addition, the simulated I-V and P-V curves are plotted to verify the GP for the reconfiguration methods, as shown in Fig.11. The parameters such as GMPP, fill-factor, efficiency and shadow loss are estimated from the figures and represented in Fig.12. It is

observed from the shading results that the proposed adaptive system is increased power output as compared to other PV arrays.

7. Comprehensive study on current reconfiguration methods

In the present scenario, various techniques of reconfiguration for the TCT array were developed and implemented in the literature. In [10], a reconfiguration of an electrical array (EAR) is formed to maintain equivalent row currents in the TCT array under PS. The EAR technique will build rows of PV modules that have the same irradiance in this work, thus improving the current of an array. This method needed more sensors and switches that would increase the cost of the system. A similar method is presented in [18] for the distribution of shading effects over the array using the PSO algorithm. During the operation of this work, the connection between PV modules is changed virtually to increase the maximum power. In [16], a one-time magic-square arrangement technique is proposed in this paper. In this work, the modules' physical positions shift without altering their connections under PS, in order to increase power output. The difficult of this method is that shifting the physical location of modules from one place to another. A verity of this method is presented in this paper to mitigate mismatch loss under PS. In this work, an adaptive based reconfiguration is proposed to hold identical rows using electrical switching and increase power efficiency. This method requires less number of sensors and switches as compared to other methods [11-15]. For a clearer appreciation, different reconfiguration methods were compared in a radar diagram (see Fig.13) with different parameters included; (A) parameters for the input, (B) payback period, (C) viability of algorithm, (D) requirement of switching components, (E) sensors requirement and (F) wiring complexity. As per the observation of the diagram tells that the diagram covering the wheel's inner diameter is the most suitable approach with higher advice while the outer diameter approaches are less adaptable to PV array reconfiguration.

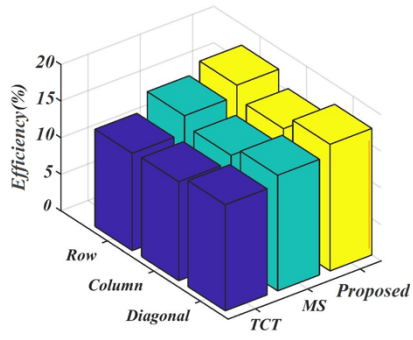

(a)

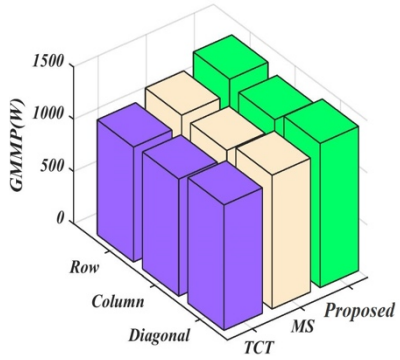

(b)

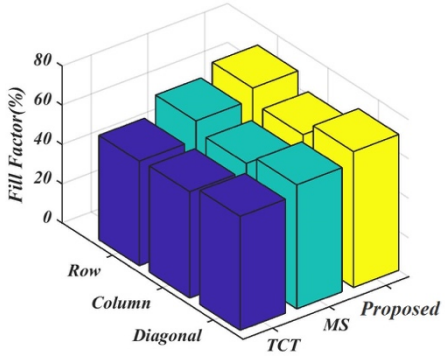

(c)

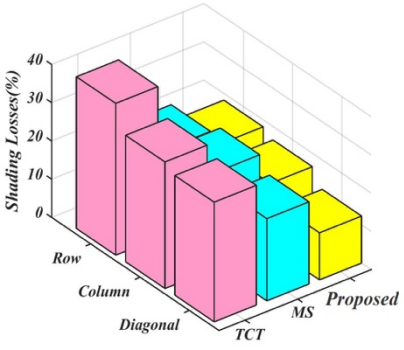

(d)

Fig.12. Estimated parameters: (a) Efficiency (%) , (b) global power output (%), (c) fill-factor (%) and (d) Shadow Loss(%)

Table 2.Possible number of connections for adaptive system under row shading.

Connections	**$F_{1(A1\ A2\ A3)}$**	**$F_{2(A1\ A2\ A3)}$**	**$F_{3(A1\ A2\ A3)}$**	**Row_1**	**Row_2**	**Row_3**	**CVI**
1	000	000	111	8.26	5.63	15.6	10.2
2	000	111	000	8.26	16.6	7.26	9.6
3	111	000	000	16.32	5.53	7.26	11.3
4	000	001	110	8.26	10.5	13.65	5.6
5	001	000	110	10.32	5.63	9.65	5.33
6	**010**	**100**	**001**	**10.32**	**10.63**	**11.65**	**1.3**
7	000	011	100	8.26	10.5	9.65	2.63
8	001	010	100	9.82	10.5	12.65	3.3
9	011	000	100	14.32	7.8	9.65	7.2
10	000	100	011	8.26	10.8	13.45	5.63
11	100	000	011	11.32	5.63	14.6	9.63
12	000	101	010	8.26	13.5	10.6	5.3
13	001	100	010	11.32	10.5	9.65	2.63
14	100	001	010	10.32	9.5	12.6	0.85
15	101	000	010	13.32	5.6	9.6	8.93
16	000	110	001	10.2	13.5	9.85	3.63
17	010	100	001	9.8	11.5	12.65	2.53
18	100	010	001	10.3	12.5	11.6	2.3
19	110	000	001	14.25	5.62	9.65	9.3
20	001	110	000	10.2	13.5	8.65	5.6
21	101	100	000	14.32	10.5	8.5	4.63
22	100	001	010	10.3	11.5	9.65	1.63
23	010	101	000	10.32	14.8	7.6	7.3
24	011	100	000	14.6	12.5	7.6	6.9
25	100	011	000	10.2	13.5	7.6	6.6
26	101	010	000	14.5	10.2	7.6	6.3
27	110	001	000	14.8	10.2	7.6	6.8

Table 3.Power generated by the adaptive connections under row shading.

Connections	2	**6**	13	18	20	22
Poweroutput	980	**1360**	1190	1220	1110	1225

Table 4.Power generated by the adaptive connections under Column shading.

Connections	6	10	**15**	20	22	25
Power output	996	1105	**1280**	1020	990	1210
CVI Index	7.56	4.3	**2.8**	4.8	7.7	3.3

Table 5.Power generated by the adaptive connections under Diagonal shading.

Connections	4	11	**16**	18	20	25
Power output	990	1000	**1300**	1100	886	1190
CVI Index	7.54	4.14	**2.5**	3.8	8.2	3.3

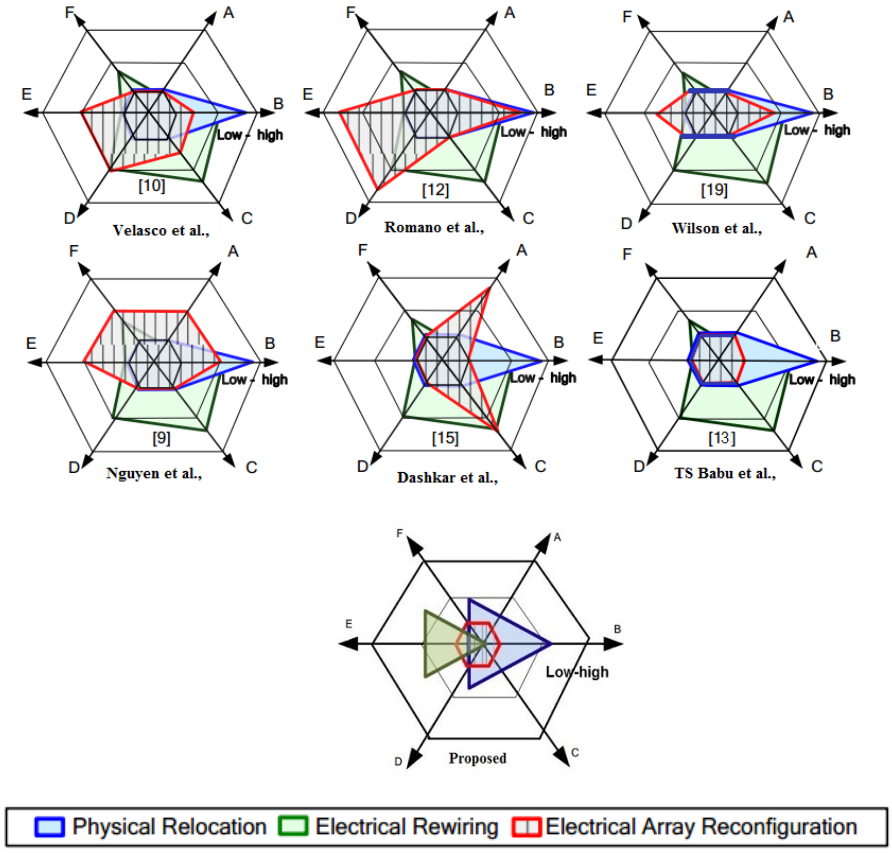

Fig.13. Radar representation of reconfiguration methods

6.1. Extension of large array sizes

The proposed adaptive reconfiguration method can be implemented by design switching matrix structure for various array sizes such as symmetric, i.e.,3×3,5×5, and asymmetric, i.e., 3×4, 4×3.

8. Conclusion

This article proposed an adaptive reconfiguration system to improve power output under partial shadings and mismatch loss. This method is implemented on 3×3 TCT array and validated under generalized shading conditions such as row, column and diagonal. Also, this adaptive method is numerically compared with the magic-square method by obtained global power output, shadow loss, and fill-factor parameters. The core findings of this paper is that the proposed adaptive method enhanced the average fill-factor and power output by 7.2% and 9.6% respectively under partial shadings as compared to other reconfiguration methods.

Acknowledgements

This research paper doesn't have any funding support.

Appendix: V_m: Photovoltaic module Voltage (V); *Im:* Photovoltaic module Current (A); V_a: Total PV array voltage (V); I_a:Total PV array current (A);V_T: Thermal voltage of diode (V); I_{ph}: Photon generated current;I_d: Diode current, I_0: Reverse saturation current; R_s, R_p: Parasitic resistances of a PV cell; N_{ss}, N_{pp}: Series and parallel connected modules;G, G_r: Actual and Reference Irradiance;A: Ideality factor; α: Shading factor, n: Ideality factor, K: Boltzmann's constant 1.38×10^{-23} J/K; q: Electron charge 1.6×10^{-19} C;i,j: Row and column index.

.

References

[1] L. L. Li, G. Q. Lin, M. L. Tseng, K. Tan, M. K. Lim, "a maximum power point tracking method for PV system with improved gravitational search algorithm", Applied Soft Computing, vol. 65, pp. 333-348, 2018.

[2] G. Meerimatha,and B. L. Rao, "Novel reconfiguration approach to reduce line losses of the photovoltaic array under various shading conditions", Energy, vol.196, pp.117120, 2020.

[3] M. A. Sameh, M. A. Badr, M. I. Mare, M. A. Attia, "Enhancing the Performance of Photovoltaic Systems under Partial Shading Conditions Using Cuttlefish Algorithm", In 2019 8th International Conference on Renewable Energy Research and Applications (ICRERA), pp.874-885, November 2019.

[4] L. F. L. Villa, D. Picault, B. Raison, S. Bacha, and A. Labonne, "Maximizing the power output of partially shaded photovoltaic plants through optimization of the interconnections among its modules", IEEE Journal of Photovoltaics, Vol. 2, No. 2, pp. 154-163, 2012.

[5] S. R. Pendem, and S. Mikkili, "Modelling, Simulation and Performance analysis of solar PV array configurations (series, series-parallel and honey-comb) to extract maximum power under partial shading conditions", Energy Reports, vol. 4, pp. 274-287, 2018.

[6] N. Karami, N. Moubayed, R. Outbib, "General review and classification of different MPPT Techniques", Renewable and Sustainable Energy Reviews, vol. 68, pp. 1-18, 2017.

[7] W. Yin, Q. Tong, Y. Xu, Y. Zhang, and Y. Zhou, "Partial Shading Impact on PV Array System and the Hard-Shading Location with BP Algorithm", In 2019 7th International Conference on Smart Grid (icSmartGrid), pp. 21-26, December 2019.

[8] G. S. Krishna and T. Moger, "Reconfiguration strategies for reducing partial shading effects in photovoltaic arrays: State of the art", Solar Energy, vol.182, pp. 429-452, 2019.

[9] D. Nguyen, and B. Lehman, "An adaptive solar photovoltaic array using model-based reconfiguration algorithm", IEEE Transactions on Industrial Electronics, vol. 55, No. 7, pp. 2644-2654, 2008.

[10] G. V. Quesada, F. G. Gispert, R. P. Lopez, M. R. Lumbreras, and A.C. Roca, "Electrical PV array reconfiguration strategy for energy extraction improvement in grid-connected PV systems", IEEE Transactions on Industrial Electronics, vol. 56, No. 11, pp. 4319-4331, 2009.

[11] G. E. N. C. Naci, and D. Haji, "Dynamic Behavior Analysis of ANFIS Based MPPT Controller for Standalone Photovoltaic Systems", International Journal of Renewable Energy Research (IJRER), vol. 10, No. 1, pp. 101-108, March 2020.

[12] P. Romano, R. Candela, M. Cardinale, V. L. Vigni, D. Musso, and E. R. Sanseverino, "Optimization of photovoltaic energy production through an efficient switching matrix" , Journal of Sustainable Development of Energy, Water and Environment Systems, Vol. 1, No. 3, pp. 227-236, 2013

[13] T. S. Babu, J. P. Ram, T. Dragičević, M. Miyatake, F. Blaabjerg, and N. Rajasekar, "Particle swarm optimization based solar PV array reconfiguration of the maximum power extraction under partial shading conditions", IEEE Transactions on Sustainable Energy, vol. 9, No. 1, pp. 74-85, 2017.

[14] Y. Tomita, Y. Nagai, M. Saito, N. Niina, and Y. Zushi, "Stable Operation of an Automotive Photovoltaic System under Moving Shadows", In 2019 8th International Conference on Renewable Energy Research and Applications (ICRERA), pp. 527-533. November 2019.

[15] O. Mesbahi, M. Tlemçani, F. M. Janeiro, A. Hajjaji, and K. Kandoussi, "A Modified Nelder-Mead Algorithm for Photovoltaic Parameters Identification", International Journal of Smart Grid (ijSmartGrid), Vol. 4, No. 1, pp. 28-37, 2020.

[16] S. Kannu, S. Mary, R. Namani, and S. K.Subramanian, "Power enhancement of partially shaded PV arrays through shade dispersion using magic square configuration", Journal of Renewable and Sustainable Energy, Vol.4, No.6, pp. 236-242, 2016.

[17] J. Solis, T. Oka, J. Ericsson, and M. Nilsson, "Forecasting of Electric Energy Consumption for Housing Cooperative with a Grid Connected PV System", In 2019 7th International Conference on Smart Grid (icSmartGrid), pp. 118-125, December 2019.

[18] M. T. Elsir, M. A. Abdulgalil, A. T. Al-Awami, and M. Khalid, "Sizing and Allocation for Solar Energy Storage System Considering the Cost Optimization", In 2019 8th International Conference on Renewable Energy Research and Applications (ICRERA), pp. 407-412, November 2019.

[19] A. Storey, P. Jonathan, R. P. Wilson, and D. Bagnall, "Improved optimization strategy for irradiance equalization in dynamic photovoltaic arrays", IEEE transactions on power electronics, Vol.28, No.6, pp. 2946-2956, 2013.